Design of the Reduced LQG Compensator for the DSS-13 Antenna

W. Gawronski
Ground Antennas and Facilities Engineering Section

A linear-quadratic-Gaussian (LQG) compensator design procedure is proposed for the DSS-13 antenna. The procedure is based on two properties. It is shown that tracking and flexible motion of the antenna are almost independent (the separation property). As a consequence, compensators for the flexible and tracking parts can be designed separately. It is shown also that the balanced LQG compensator's effort is evenly divided between the controller and the estimator. This allows a minimization of the compensator order, which is important for implementation purposes. An efficient compensator reduction procedure that gives a stable low-order compensator of satisfactory performance is introduced. This approach is illustrated with a detailed compensator design for the DSS-13 antenna. The implementation of this compensator design requires an update of the antenna model.

I. Introduction

The linear quadratic controller for the DSS-14 antenna was designed by Alvarez and Nickerson [1], and a linear quadratic controller for the DSS-13 antenna was designed by Gawronski [2]. The design method presented in this article extends the results obtained in [2] for the case when full-state feedback is not available.

The development of new high-performance controllers for the DSN antennas is a current priority. The existing proportional and integral (PI) controllers satisfy the requirements for X-band (8.4-GHz) tracking; they remain simple, robust to parameter variations, and do not require detailed knowledge of the antenna dynamics. However, due to the recent pointing requirements for Ka-band (32 GHz), new performance requirements for the antenna controllers have emerged. The PI controllers have reached their performance limits, therefore a new generation of controllers has to be designed and developed. Also, in order to improve controller performance, more sophisticated and accurate antenna models have to be developed. As a rule, the better the knowledge of the plant dynamics, the better the performance that can be achieved by the controller. The recently developed antenna models [3] are accurate enough to give an opportunity to improve tracking performance. The models allow simulation of simultaneous tracking in azimuth and elevation, and include antenna flexible deformations up to 10 Hz.

Among the family of the model-based controllers, the linear-quadratic-Gaussian (LQG) compensator has been chosen for the DSN antennas because it is commonly known to be performing well in industrial applications. The LQG compensator consists of a controller and an estimator. The controller drives the antenna, and the driving control torques are determined from the knowledge of the full antenna dynamics. Since only a small part of the antenna dynamics is measured (by encoders), the estimator is implemented to reconstruct the "missing" dynamics.

The controller and the estimator designs consist of adjusting their gains through proper determination of the controller and estimator weights. For the antenna model of order n, $2n^2$ weights have to be determined (n^2 for the controller and n^2 for the estimator). This number is customarily dropped to $2n$ weights (n for the controller and n for the estimator). But in spite of this drastic reduction, the number of weights is still too large to make the search for the best weights reasonable (typically $n = 40$ for the antenna, i.e., 80 weights have to be found). The difficulty arises because no general procedure for weight determination is available, and the known procedures deal with simplified and/or specific cases.

The weight determination presented here becomes simple due to several properties of the antenna and the compensator investigated in this article. First, it is shown that the tracking and flexible motion of the antenna are almost separated. The tracking part consists of four states (elevation and azimuth encoder readings and their integrals); thus, instead of dealing with a model of order n, one obtains two separate models of order 4 and $n - 4$. Secondly, the LQG compensator is balanced such that the controller and compensator efforts are the same. For the balanced compensator, the weights of the controller and estimator are the same, thus instead of $2n$ weights, n weights need to be determined. Thirdly, it is shown that each component of the balanced compensator (consisting of two states) is almost independent of others. Thus, weights for each component are determined separately. In consequence, the search for $2n$ weights becomes a series of searches for 2 weights, which obviously is not a difficult task to perform.

As mentioned, the PI controller is easy to implement due to its simplicity. But the implementation of the 40-state model-based LQG compensator is not an easy task. It would result in a complex algorithm, and would be a huge computational burden. Therefore, a simplification of the LQG compensator is an important implementation requirement. The simplification is obtained through order reduction of the compensator. The size of the compensator is reduced, but one has to find a reduction procedure such that the reduced-order compensator is stable and its performance is still close to the full-order compensator. This task is solved by introducing the pole mobility index. The pole mobility index characterizes the importance of the components of the balanced compensator. The states with small pole mobility index are truncated, and the truncation marginally affects the closed-loop dynamics. The closed-loop system with the reduced compensator is stable, and its performance is close to the full-order compensator. It is shown that the reduced-order compensator of 12 states is stable and its performance is close to the performance of the full-order compensator of 40 states.

II. Problem Statement

The closed-loop system with an LQG compensator is shown in Fig. 1, with the plant state-space triple (A, B, C), the process noise v of intensity V, and the measurement noise w of intensity W, where both v and w are uncorrelated:

$$V = E(vv^T), \quad W = E(ww^T)$$
$$E(vw^T) = 0, \quad E(v) = 0, \quad E(w) = 0 \tag{1}$$

where $E(.)$ is an expectation operator. It is assumed that $W = I$ without loss of generality. The task is to determine the controller gain (K_p) and estimator gain (K_e) such that the performance index J

$$J = E\left(\int_0^\infty (x^T Q x + u^T R u) dt\right) \tag{2}$$

is minimal, where R is a positive definite input weight matrix, and Q is a positive semidefinite state weight matrix. It is assumed that $R = I$, also without loss of generality. The minimum of J is obtained for the feedback $u = -K_p x$, where the gain matrix

$$K_p = B^T S \tag{3}$$

is obtained from the solution S of the controller Riccati equation (CARE) [4,5]:

$$A^T S + SA - SBB^T S + Q = 0 \tag{4}$$

The optimal estimator gain is given by

$$K_e = PC^T \tag{5}$$

where P is the solution of the estimator Riccati equation (FARE):

$$AP + PA^T - PC^T CP + V = 0 \tag{6}$$

The LQG compensator performance can be significantly modified through variations of weight Q and variance V. Although V is formally predetermined by the process noise v, it can be modified in a search for a more suitable solution [5,6]. The determination of the weight and covariance is addressed in the following section.

Another nontrivial issue addressed here is the order of the compensator. Although the size of the plant determines the size of the compensator, in many cases a full-size compensator is not acceptable for implementation due to its complexity. Thus, its order must be minimized in such a way that the reduced compensator maintains the stability and performance of the full-order compensator. The solution to this problem is found through the approximate balancing of the CARE/FARE equations.

III. Quasi-Separation of Flexible and Tracking Subsystems

The open-loop (or rate-loop) state-space representation (A, B, C) of the DSS-13 antenna includes the input $u_p^T = [u_{pe}\ u_{pa}]$, which consists of the rate commands in elevation (u_{pe}) and azimuth (u_{pa}) and the outputs $y_p^T = [y_{pe}\ y_{pe}]$ and $y_i^T = [y_{ie}\ y_{ia}]$, which consist of the elevation and azimuth angles $(y_{pe},\ y_{pa})$ and their integrals $(y_{ie},\ y_{ia})$. Divide the state vector x of the open-loop antenna model into the tracking x_t and flexible x_f parts

$$x^T = [x_t^T \quad x_f^T] \tag{7}$$

where $x_t^T = [y_i^T \quad y_p^T]$ and x_f are the remaining states. It can be shown [2] that, in this case, the rate-loop representation (A, B, C) has the form

$$A = \begin{bmatrix} A_t & A_{tf} \\ 0 & A_f \end{bmatrix}, \quad B = \begin{bmatrix} B_t \\ B_f \end{bmatrix}, \quad C = [C_t \quad 0] \tag{8}$$

and that

$$\| B_t \| \ll \| B_f \|, \ \| A_{tf} \| \ll \| A_t \|, \ \| A_{tf} \| \ll \| A_f \| \tag{9}$$

For the DSS-13 antenna, $\| B_t \| < 10^{-5}$, $\| B_f \| > 1$, $\| A_{tf} \| < 10^{-3}$, $\| A_f \| > 10$, and $\| A_t \| = 1$. Thus, the states of the tracking part are much weaker than the states of the flexible part. The strong and weak signal flow is shown in the block diagram of Fig. 2. The strong states of the flexible subsystem and the weak states of the tracking subsystem are shown in Fig. 3, which presents the transfer function plots of the rate-loop systems due to elevation rate command.

In the LQG design, the performance index is minimized and the minimum is obtained for $K = B^T S$, and S is a solution of the Riccati Eq. (4). Divide S and K into parts related to the triple (A, B, C) in Eq. (8)

$$S = \begin{bmatrix} S_t & S_{tf} \\ S_{tf}^T & S_f \end{bmatrix}, \quad K = [K_t\ K_f] \tag{10}$$

so that Eq. (4) can be written as follows

$$A_t^T S_t + S_t A_t - S_t B_t B_t^T S_t + Q_t - \Delta_{tf} = 0 \tag{11a}$$

$$A_t^T S_{tf} + S_{tf} A_f + S_t A_{tf} - K_t^T K_f = 0 \tag{11b}$$

$$A_f^T S_f + S_f A_f + S_f B_f B_f^T S_f + Q_f - \Delta_{ft} = 0 \tag{11c}$$

where

$$\left.\begin{aligned} \Delta_{ft} &= A_{tf}^T S_{tf} + S_{tf}^T A_{tf} - S_{tf}^T B_t K_f \\ &\quad + S_f B_f B_t^T S_{tf} \\ \Delta_{tf} &= S_t B_t B_f^T S_{tf}^T + S_{tf} B_f K_t \end{aligned}\right\} \tag{12a}$$

$$K_f = B_t^T S_{tf} + B_f^T S_f, \quad K_t = B_t^T S_t + B_f^T S_{tf}^T \tag{12b}$$

Taking a closer look at Eqs. (12), notice that there exist weights Q_t and Q_f such that the gain K_f depends on the flexible subsystem only. Namely, for large enough Q_f, such that $\| Q_f \| \gg \| \Delta_{ft} \|$, the solution S_f of Eq. (11c) is independent of the tracking system, and for small Q_t, one obtains $\| B_t^T S_{tf} \| \ll \| B_f^T S_f \|$. In terms of Eq. (12a), the latter inequality means that the gain K_f depends only on the flexible subsystem. However, due to the master-slave relationship between flexible and tracking subsystems, the situation is not quite symmetric: There are no such Q_t and Q_f that the gain K_t depends only on the tracking subsystem. To understand this, note that the term "small" has a different meaning for Q_f and Q_t. Magnitudes of small Q_f and small Q_t are of different order, namely small Q_f is such that $Q_f < 10^{-7}$, and small Q_t is such that $Q_t < 1$. Therefore, by increasing Q_t in order to obtain $\| Q_t \| \gg \| \Delta_{tf} \|$ one obtains $\| B_f^T S_{ft} \|$ and $\| B_t^T S_t \|$ of the same magnitude. According to Eq. (12b), the latter fact means that the gain K_t depends on the flexible subsystem, as well as on the tracking subsystem, and the solution S_t of Eq. (11a) is dependent on the flexible subsystem. This property can be validated by observation of the closed-loop transfer functions for different weights (Fig. 4). The plots show that the variations of Q_f changed the properties of the flexible subsystem only, while the variations of Q_t changed the properties of both subsystems.

The weight Q_t should be large enough to achieve the pointing performance requirements, and the increase of Q_t

causes increasing dependency of the gains on the tracking system. For this reason the above independence becomes a quasi-independence in the final stage of controller design. Nevertheless, the separation in the initial stages of controller design is very strong. The design consists, therefore, of the initial choice of relatively small weights for the tracking subsystem and determination of the controller gains of the flexible subsystem. It is followed by adjustment of weights of the tracking subsystem and a final tuning of the flexible weights.

The quasi-separation principle discussed above in the case of the controller design is also valid in the case of estimator design, since the compensator design consists of the independent designs of a controller and an estimator [4,5]. Additional properties of the LQG compensator that arise in controls of flexible structures are discussed in the following section.

IV. Balanced LQG Compensator for Flexible Structures

In this section the flexible subsystem is considered only (subscript "f" is dropped in this section for simplicity of notation). A flexible structure is defined as a controllable and observable linear system with distinct complex conjugate pairs of poles (N poles, N is even) and with small real parts of the poles. In other words, it is a linear system with vibrational properties. In the Moore balanced coordinates, it consists of $n = N/2$ components [7,8], and each component consists of two states.

An approximately balanced LQG compensator is considered. An approximate equality between two variables is used in the following sense: Two variables x and y are approximately equal ($x \cong y$) if $x = y + \epsilon$, and $\|\epsilon\|/\|y\| \ll 1$.

The block diagram of a closed-loop flexible system with the LQG compensator is shown in Fig. 5. Similar to the balancing of controllability and observability grammians is the balancing of CARE and FARE equations. Namely, there exists a diagonal positive definite $M = diag\,(\mu_i)$, $i = 1, ..., n, \mu_i > 0$, such that

$$S = P = M \tag{13}$$

A state-space representation with the condition Eq. (13) satisfied is called an LQG balanced representation, and μ_i, $i = 1, ..., n$ represents the characteristic values of (A, B, C). Jonckheere and Silverman [9] and Opdenacker and Jonckheere [10] have shown that a balanced solution for CARE and FARE equations exists in the case of $Q = C^T C$ and $V = BB^T$. Gawronski [11] has shown that the balanced LQG representation exists in the case of general Q and V, and has derived the transformation to the balanced LQG representation.

Let (A, B, C) be a state-space triple of an open-loop system. Its controllability and observability grammians W_c and W_o are positive-definite and satisfy the Lyapunov equations

$$\begin{aligned} AW_c + W_c A^T + BB^T &= 0 \\ A^T W_o + W_o A + CC^T &= 0 \end{aligned} \tag{14}$$

The system representation is balanced in the sense of Moore [12] if its controllability and observability grammians are diagonal and equal:

$$W_c = W_o = \Gamma^2, \quad \Gamma = diag(\gamma_1, ..., \gamma_N), \quad i = 1, ..., N \tag{15}$$

where $\gamma_i > 0$ is the ith Hankel singular value of the system. In [11] it is shown that, for flexible structures, the balanced representation (in the Moore sense) produces diagonally dominant solutions of CARE and FARE, and in the case of $Q = V$ produces approximate LQG balanced solutions S and P, such that $S \cong P \cong M$. Assume a diagonal weight matrix Q:

$$Q = diag(q_i I_2), \qquad i = 1, ..., n \tag{16}$$

Then there exists $q_i \leq q_{oi}$, where $q_{oi} > 0$, $i = 1, ..., n$, such that $S \cong diag\,(s_i I_2)$ is the solution of Eq. (4), where

$$s_i = (\beta_{pi} - 1)/2\gamma_i^2, \quad \beta_{pi}^2 = 1 + 2q_i\gamma_i^2/\zeta_i\omega_i \tag{17}$$

The proof is presented in the Appendix. The plots of s_i with respect to q_i and γ_i are shown in Fig. 6. They show an increase of s_i with the increase of weight q_i, and decrease of s_i with increase of γ_i^2 or $\zeta_i\omega_i$.

A similar result is obtained for the FARE equation, namely, for a diagonal V:

$$V = diag(v_i I_2), \quad i = 1, ..., n \tag{18}$$

there exists $v_i \leq v_{oi}$, where $v_{oi} > 0$, $i = 1, ..., n$, such that $P \cong diag(p_i I_2)$ is the solution of Eq. (6), where

$$p_i = (\beta_{ei} - 1)/2\gamma_i^2, \quad \beta_{ei}^2 = 1 + 2v_i\gamma_i^2/\zeta_i\omega \tag{19}$$

If the ith diagonal entry of P and the respective entry of S are equal, say to μ_i, i.e.,

$$p_i = s_i = \mu_i \tag{20}$$

the ith component is LQG balanced; if S and P are equal the system is LQG balanced. If S, P, and M are diagonally dominant, i.e. $v_i + \epsilon_{vi} \cong s_i + \epsilon_{si} \cong \mu_i$, with ϵ_{vi} and ϵ_{si} small ($|\epsilon_{vi}/v_i| \ll 1, |\epsilon_{si}/s_i| \ll 1$), the system is approximately LQG balanced.

It follows from Eqs. (17) and (19) that for $Q = diag(q_i) = V = diag(v_i)$, the system is approximately LQG balanced, such that

$$\begin{aligned} &S \cong P \cong M = diag(\mu_i) \\ &\mu_i = (\beta_i - 1)/2\gamma_i^2, \quad \beta_i^2 = 1 + 2q_i\gamma_i^2/\zeta_i\omega \end{aligned} \tag{21}$$

Next it is shown that the weight Q

$$Q = diag(0, 0, ..., q_iI_2, ...0, 0), \quad q_i \leq q_{oi} \tag{22}$$

shifts the ith pair of complex poles of flexible structure, and leaves the remaining pairs of poles almost unchanged. Only the real part of the pair of poles is changed (just moving the pole apart from the imaginary axis and stabilizing the system), and the imaginary part of the poles remains unchanged. Namely, for the weight Q as in Eq. (22), the closed-loop pair of flexible poles (λ_{cri}, $\pm j\lambda_{cii}$) relates to the open-loop poles (λ_{ori}, $\pm j\lambda_{oii}$) as follows:

$$(\lambda_{cri}, \pm j\lambda_{cii}) \cong (\beta_{pi}\lambda_{ori}, \pm j\lambda_{oii}), \quad i = 1, ..., n \tag{23}$$

where β_{pi} is defined in Eq. (17). The proof is presented in the Appendix.

The real part of the poles is shifted by β_{pi}, while the imaginary part remains unchanged. The above proposition has additional interpretations. Denote the real part of the open-loop pole by $\lambda_{ori} = -\zeta_i\omega_i$ and the real part of the closed-loop pole by $\lambda_{cri} = -\zeta_{ci}\omega_i$; note also that the height of the open-loop resonant peak is $\alpha_{oi} = \kappa/2\zeta_i\omega_i$, where κ is a constant, and the closed-loop resonant peak is $\alpha_{ci} = \kappa/2\zeta_{ci}\omega_i$. From Eq. (23), $\beta_{pi} = \lambda_{cri}/\lambda_{ori}$; thus, one obtains

$$\beta_{pi} = \zeta_{ci}/\zeta_i = \alpha_{oi}/\alpha_{ci} \tag{24}$$

i.e., β_{pi} is a ratio of closed- and open-loop damping factors, or it is a ratio of open- and closed-loop resonant peaks. Therefore, if a suppression of the ith resonant peak by the factor β_{pi} is required, the appropriate weight q_i is determined from Eq. (17):

$$q_i = 0.5(\beta_{pi}^2 - 1)\zeta_i\omega_i\gamma_i^{-2} \tag{25}$$

An alternative interpretation of β_i is as a ratio of the open-loop Hankel singular value to the closed-loop Hankel singular value:

$$\beta_i = \gamma_{oi}^2/\gamma_{ci}^2 \tag{26a}$$

or a ratio of variances of open-loop (σ_{oi}^2) and closed-loop (σ_{ci}^2) states excited by the white-noise input [13]:

$$\beta_i = \sigma_{oi}^2/\sigma_{ci}^2 \tag{26b}$$

The proof is presented in the Appendix.

The plots of β_{pi} with respect to q_i and γ_i are shown in Fig. 7. They show relatively large β_{pi} even for small q_i, i.e., a significant pole shift to the left. Also, β_{pi} increases with the increase of γ_i, and decreases with the increase of $\zeta_i\omega_i$, i.e., there is a significant pole shift for highly observable and controllable states with small damping. In terms of the transfer function profile, the weight q_i suppresses the resonant peak at frequency ω_i while leaving the natural frequency unchanged. Due to weak coupling between the states, the assignment of one pair of states does not significantly impact other states. Thus, the weight assignment can be done separately for each pair of states.

The estimator poles are shifted in a similar manner. Denote

$$V = diag(0, 0, ..., v_iI_2, ...0, 0), \quad v_i \leq v_{oi} \tag{27}$$

then for the weight V as in Eq. (27) and $v_i \leq v_{oi}$, the estimator pair of poles (λ_{eri}, $\pm j\lambda_{eii}$) relates to the open-loop poles (λ_{ori}, $\pm j\lambda_{oii}$) as follows:

$$(\lambda_{eri}, \pm j\lambda_{eii}) \cong (\beta_{ei}\lambda_{ori}, \pm j\lambda_{oii}), \quad i = 1, ..., n \tag{28}$$

where β_{ei} is defined in Eq. (19).

The limiting values q_{oi} and v_{oi} are determined. Their values are rather fuzzy numbers. Despite their fuzziness, they are not difficult to determine. There are several indicators that q_i is approaching q_{oi}, or that v_i is approaching v_{oi}. For the controller, q_{oi} is the weight for which the ith pair of complex poles of the plant departs from the horizontal trajectory in the root-locus plane, or it is the weight for which the ith resonant peak of the plant transfer function disappears (the peak is flattened). For the estimator, v_{oi} is the covariance for which the ith pair of complex poles of the estimator departs from the horizontal trajectory in the root-locus plane, or it is a covariance for which the ith resonant peak of the estimator transfer function disappears.

It is crucial from an implementation point of view to obtain a compensator of the smallest possible dimension that preserves the stability and performance of the full-order compensator. Although the size of a plant determines the size of a compensator, the plant model cannot be reduced excessively in advance in order to assure the quality of the closed-loop system. Therefore, compensator reduction is a part of the compensator design. The balanced LQG design procedure provides this opportunity.

To successfully perform the compensator reduction, an index of the importance of each compensator component is introduced. In the open-loop case, Hankel singular values serve as reduction indices. In the closed-loop case, the characteristic values of the system seem to be good candidates for the reduction indices, as suggested in [9]. This is not a good choice, however, since the characteristic values do not properly reflect the effectiveness of the compensator. The effectiveness of the closed-loop system can be evaluated by the relative suppression of the closed-loop output when compared to the open-loop output. Thus, the ratio of variances of the closed-loop output and the open-loop output excited by the white noise input is an appropriate measure of the suppression (alias the compensator performance). It will be shown later that the suppression depends on pole mobility in the complex plane. Therefore, if a particular pair of poles is easily moved (i.e., in the case when small weight is required), the respective states are easy to control and to estimate. On the contrary, if a particular pair of poles is difficult to move (i.e., a large weight is required to move the poles), the respective states are difficult to control and to estimate. In the latter case, the action of the compensator is irrelevant, and the states that are difficult to control and estimate can be reduced; thus, pole mobility is a good indicator of the importance of a particular compensator state.

Consider an LQG balanced system, and denote the pole mobility index π_i by

$$\pi_i = 0.5(\beta_i - 1) \tag{29}$$

Note that for $\beta_i = 1$, the ith pole is stationary and π_i is equal to zero; for a shifted pole, one obtains $\beta_i > 1$ and $\pi_i > 0$. If for small π_i a small pole shift (in plant, as well as in estimator) is observed, this component can be reduced.

Another useful interpretation follows from Eqs. (29) and (26):

$$\pi_i = 0.5(\gamma_{oi}^2 - \gamma_{ci}^2)/\gamma_{ci}^2 = 0.5(\sigma_{oi}^2 - \sigma_{ci}^2)/\sigma_{ci}^2 \tag{30}$$

i.e., the pole mobility index is proportional to the relative change in the white noise response of the open- and closed-loop systems. Furthermore, from Eqs. (21) and (29), it can be shown that the pole mobility index is a product of the square of a Hankel singular value and the characteristic value of the system:

$$\pi_i = \gamma_i^2 \mu_i \tag{31}$$

Thus, π_i combines the system observability and controllability properties of the open-loop system with the closed-loop performance. The more heavily weighted the component, the larger its pole mobility index, see Fig. 8(a). Also, the larger the Hankel singular value of the component, the larger the corresponding pole mobility index, c.f. Fig. 8(b).

The matrix Π of pole mobility indices is defined as

$$\Pi = diag(\pi_1, \pi_2, ..., \pi_{n-1}, \pi_n) \tag{32}$$

and it is obtained from Eqs. (15) and (29) as

$$\Pi = \Gamma^2 M \tag{33}$$

In the following, a reduction technique is discussed. Assume Π in Eq. (32) has a descending order, i.e., $\pi_i \geq 0$, $\pi_{i+1} \leq \pi_i$, $i = 1, ..., n$, and divide Π as follows:

$$\Pi = diag(\Pi_r, \Pi_t) \tag{34}$$

where Π_r consists of the first k entries of Π, and Π_t the remaining ones. If the entries of Π_t are small in comparison with the entries of Π_r, the compensator is reduced by truncating its last $n - k$ states.

It is shown in [11] that a system with the reduced-order compensator obtained by reducing states with small Π_t *is expected* to be stable. That is, although it is not guaranteed, there is a well-founded expectation to obtain a stable system with the reduced-order compensator. Also, the estimation errors of the full-order and reduced-order compensators are approximately the same.

V. Closed-Loop System

The LQG compensator configuration for the DSN antenna is shown in Fig. 1. The tracking command y_c is compared with the estimated antenna position $\hat{y}_p$, and the error $e = \hat{y}_p - y_c$ along with the integral e_i of the error e are the plant inputs. The equations for the integrator, plant, and the estimator are, respectively,

$$\dot{e}_i = e \tag{35a}$$

$$\dot{x} = Ax + Bu, \quad y_p = C_p x, \quad x_f = C_f x \tag{35b}$$

$$\dot{\hat{x}} = A\hat{x} + Bu + K_e(y_p - C_p\hat{x}) \tag{35c}$$

$$u = -K_f\hat{x}_f - K_p e - K_i e_i$$

Denoting $x_{cl}^T = [e_i^T \quad x^T \quad \hat{x}^T]$, one obtains

$$\dot{x}_{cl} = A_{cl}x_{cl} + B_{cl}y_c, \quad y = C_{cl}x_{cl} \tag{36a}$$

where

$$A_{cl} = \begin{bmatrix} 0 & 0 & C_p \\ -BK_i & A & -BK_fC_f - BK_pC_p \\ -BK_i & K_eC_p & A - BK_fC_f - BK_pC_p - K_eC_p \end{bmatrix}, \quad B_{cl} = \begin{bmatrix} -I \\ BK_p \\ BK_p \end{bmatrix}, \quad C_{cl} = [0 \quad C_p \quad 0] \tag{36b}$$

The triple $(A_{cl},\ B_{cl},\ C_{cl})$ for the LQG system with the reduced-order estimator $(A_r,\ B_r,\ C_r)$ is as follows:

$$A_{cl} = \begin{bmatrix} 0 & 0 & C_p \\ -BK_i & A & -BK_fC_{fr} - BK_pC_{pr} \\ -B_rK_i & K_{er}C_p & A_r - B_rK_fC_{fr} - B_rK_pC_{pr} - K_{er}C_{pr} \end{bmatrix}, \quad B_{cl} = \begin{bmatrix} -I \\ BK_p \\ B_rK_p \end{bmatrix}, \quad C_{cl} = [0 \quad C_p \quad 0] \tag{37}$$

where C_{pr} and C_{fr} are obtained from the partition of C_r, $C_r = [C_{pr} \quad C_{fr}]$.

VI. Compensator Design Algorithm

Weights for the balanced LQG controller and estimator are identical. Therefore, in the algorithm, the controller and estimator gains are adjusted simultaneously. The procedure for the antenna LQG compensator design is a sequential one. First, for the ad hoc (but relatively small) chosen tracking subsystem weights, the flexible subsystem weights are determined (recall that the controller and estimator weights are the same). Second, the adjustment of the tracking system weights is performed, followed by final adjustment of the flexible system weights. The flexible subsystem weights are determined sequentially, which gives more insight into the system performance and simplifies the procedure.

The estimator order is determined as a part of the weight tuning process. Only the modes with large index π_i are considered. If the number of flexible modes is n_f, the number of disregarded modes is n_o, and the size of the tracking system is n_t, then the controller order n_c is $n_c = n_t + 2(n_f - n_o)$. The following LQG compensator design algorithm is proposed:

(1) Determine the plant state-space representation in the form of Eq. (8), consisting of flexible and tracking parts.

(2) Choose ad hoc but reasonably small weights and variances for the tracking part $Q_t = V_t = Q_{\text{tah}}$.

(3) For each balanced coordinate of the flexible part, choose the weight q_i, $i = 1, ..., n_f$, and define the weight and covariance matrices $Q_{fi} = diag\ (0, 0, ..., q_i, q_i, 0, 0, ...0)$, $V_{fi} = Q_{fi}$ so that the closed-loop system performance for the weight $Q_i = diag(Q_{\text{tah}}, Q_{fi})$ and the covariance $V_i = Q_i$ is optimized. For example, determine the weights q_i to impose the required pole shift or to suppress the ith resonant peak to the required level without depreciating other properties of the closed-loop transfer function. Note that for small q_i, only the ith pair of poles is shifted (to the left), and the remaining poles are almost unaffected. Disregard the modes with small index π, for which the weighting does not improve the closed-loop system performance.

(4) For the already determined Q_f and V_f, tune weight Q_t and assume covariance $V_t = Q_t$ to obtain improvements in tracking properties of the antenna.

(5) Adjust flexible subsystem weights, if necessary.

VII. Applications

A balanced LQG compensator was designed for the DSS-13 antenna. The DSS-13 antenna model consists of two tracking states (azimuth and elevation angle) and 13 flexible modes (or 26 balanced states). The preliminary weights $q_{ie} = q_{pe} = q_{ia} = q_{pa} = 1$ for the tracking subsystem (for y_i and y_p) and zero weights for the flexible subsystem ($q_1 = q_2 = ... = q_{13} = 0$ for all 13 modes) were chosen. The closed-loop system step response is presented in Fig. 9 (azimuth encoder reading due to azimuth command) and the magnitudes of the closed-loop transfer function in Fig. 10. Both figures show that flexible motion of the antenna is excessive and should be damped out. This is achieved by adjusting weights for the flexible subsystem. For the tracking weights as before, the weight for the first mode (2.32 Hz) is chosen to be $q_1 = 10^{-7}$, and the remaining weights are zero, obtaining the closed-loop system responses as shown in Figs. 11 and 12. One can see that the 2.32-Hz resonance peak in the azimuth command response (Fig. 11) has disappeared, along with most of the flexible motion in the azimuth step response (Fig. 12). The elevation motion is unaffected, however, since the azimuth mode is almost nonexistent in the elevation motion.

The weight should be chosen carefully. Weight that is too small (e.g., 3×10^{-9} in the case considered) will not suppress the resonant peak, Fig. 13(a). Weight that is too large (e.g., 10^{-5}) will deteriorate the tracking performance: for the overweighted mode the transfer function is pressed down within a wide frequency range, Fig. 13(b). The proper weight suppresses the resonant peak, leaving the other peaks unchanged.

Similar procedures have been applied for the second (2.64-Hz), third (4.26-Hz), fourth (3.77-Hz), fifth (7.92-Hz), sixth (4.47-Hz), seventh (3.38- Hz), eighth (5.98-Hz), ninth (7.32-Hz), and tenth (9.48-Hz) modes, with weight 10^{-7} for each mode. As a result, the suppression of the remaining flexible motion is observed as shown in Fig. 14. Weights for the remaining modes (eleventh through thirteenth) have been set to zero.

The root locus of the closed-loop system due to weight variations of the 7.92-Hz (fifth) mode is shown in Fig. 15. The figure shows the horizontal departure of poles to the left (stabilizing property). It confirms the properties of the weighted LQG design described previously.

In the next step, the tracking properties of the system are improved by proper weight setting of the tracking subsystem. Namely, setting the integral weight to $q_{ie} = q_{ia} = 70$ and the proportional weight to $q_{pe} = q_{pa} = 100$ improves the system tracking properties, as shown in Fig. 16 (small overshoot and settling time) and in Fig. 17 (extended bandwidth up to 2 Hz). However, by improving the tracking properties, the transfer function has been raised dramatically in the frequency region of 1 to 3 Hz, which forces the first two modes located in this region to appear again in the step response. By sacrificing a bit of the tracking properties, the flexible motion in the step response is removed. This is done by slightly increasing the weights of the flexible subsystem, setting them as follows: $q_1 = q_2 = q_3 = q_4 = q_5 = q_6 = 10^{-6}$, $q_7 = q_8 = 10^{-7}$, and $q_9 = q_{10} = 10^{-5}$. The closed-loop system response with satisfactory tracking performance is shown in Figs. 18 and 19 (small overshoot, settling time, and 1-Hz bandwidth are observed).

The reduced-order compensator is obtained through evaluation of pole mobility indices π_i. The plot of π_i is shown in Fig. 20. Reducing the order of the estimator to 12 states [the first four are tracking states (states 1 to 4), the next six are flexible states (states 5 to 10), and the last two states are nonflexible components of the rate loop model (states 25 and 27)] gives the stable and accurate closed-loop system. The reduced-order compensator is compared with the full-order compensator in the step response plots in Fig. 21, and the transfer function plots in Fig. 22, showing satisfactory approximation.

VIII. Conclusions

A method for designing a reduced-order compensator for the DSS-13 antenna has been presented. A balanced LQG compensator has been introduced that uses the same amount of effort to control and to estimate the system.

The properties of the balanced LQG system are used to obtain a reduced-order compensator for the antenna. This compensator preserves the stability and performance of the full-order compensator. The performance of the reduced-order compensator has been verified by simulations.

References

[1] L. S. Alvarez and J. Nickerson, "Application of Optimal Control Theory to the Design of the NASA/JPL 70-Meter Antenna Axis Servos," *TDA Progress Report 42-97*, vol. January–March 1989, Jet Propulsion Laboratory, Pasadena, California, pp. 112–126, May 15, 1989.

[2] W. Gawronski, "Sequential Design of a Linear Quadratic Controller for the Deep Space Network Antennas," *Proceedings of the 1992 AIAA Guidance, Navigation, and Control Conference*, Hilton Head, South Carolina, pp. 1399–1408, 1992.

[3] W. Gawronski and J. A. Mellstrom, "Modeling and Simulations of the DSS 13 Antenna Control System," *TDA Progress Report 42-106*, vol. April–June 1991, Jet Propulsion Laboratory, Pasadena, California, pp. 205–248, August 5, 1991.

[4] H. Kwakernaak and R. Sivan, *Linear Optimal Control Systems*, New York: Wiley-Interscience, 1972.

[5] B. D. O. Anderson and J. B. Moore, *Optimal Control*, Englewood Cliffs, New Jersey: Prentice Hall, 1990.

[6] J. M. Maciejowski, *Multivariable Feedback Design*, Wokingham, England: Addison–Wesley, 1989.

[7] W. Gawronski and J.-N. Juang, "Model Reduction for Flexible Structures," *Control and Dynamics Systems*, edited by C. T. Leondes, vol. 36, New York: Academic Press, pp. 143–222, 1990.

[8] W. Gawronski and T. Williams, "Model Reduction for Flexible Space Structures," *J. of Guid. Control Dyn.*, vol. 14, no. 1, pp. 68–76, January 1991.

[9] E. A. Jonckheere and L. M. Silverman, "A New Set of Invariants for Linear Systems—Application to Reduced Order Compensator Design," *IEEE Trans. Autom. Control*, vol. AC-28, no. 10, pp. 953–964, 1983.

[10] P. Opdenacker and E. A. Jonckheere, "LQG Balancing and Reduced LQG Compensation of Symmetric Passive Systems," *Int. J. Control*, vol. 41, no. 1, pp. 73–109, 1985.

[11] W. Gawronski, "Balanced LQG Compensator for Flexible Structures," *Proceedings of the 1993 IEEE American Control Conference*, San Francisco, June 1993.

[12] B. C. Moore, "Principal Component Analysis in Linear Systems: Controllability, Observability and Model Reduction," *IEEE Trans. Autom. Control*, vol. 26, pp. 17–32, 1981.

[13] W. Gawronski and H. G. Natke, "Balancing Linear Systems," *Int. J. Sys. Sci.*, vol. 17, pp. 237–249, 1987.

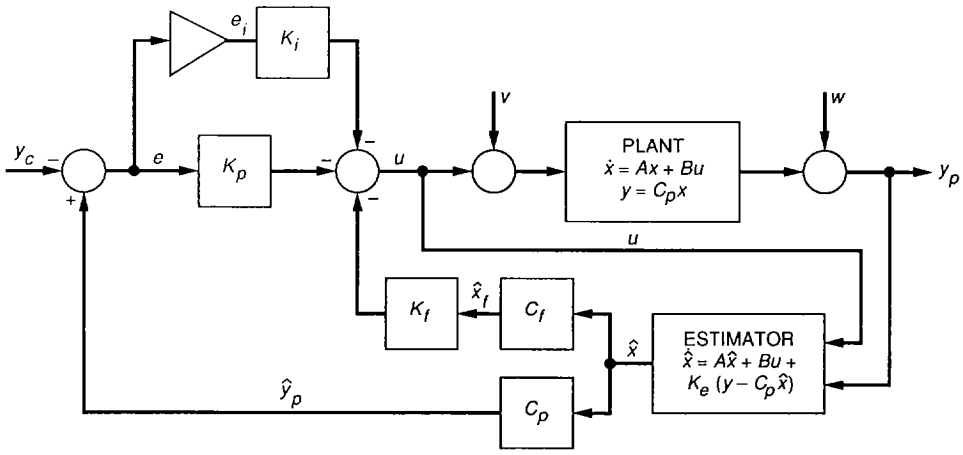

Fig. 1. LQG compensator configuration for DSS-13 antenna.

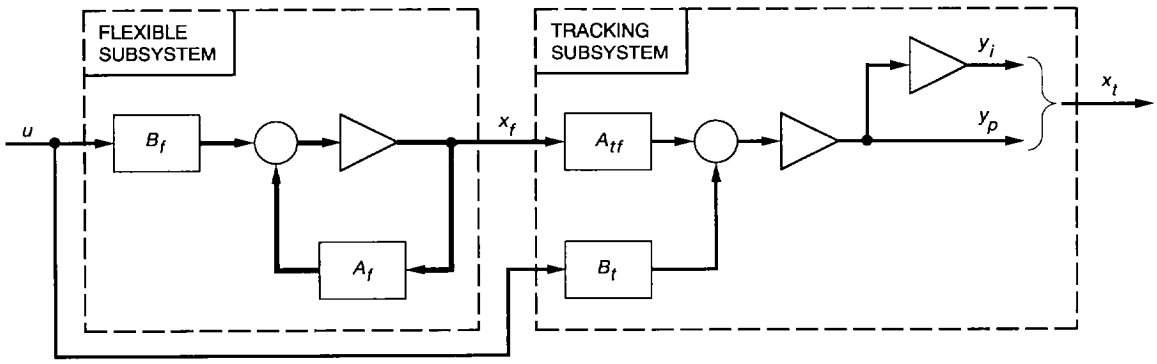

Fig. 2. System configuration.

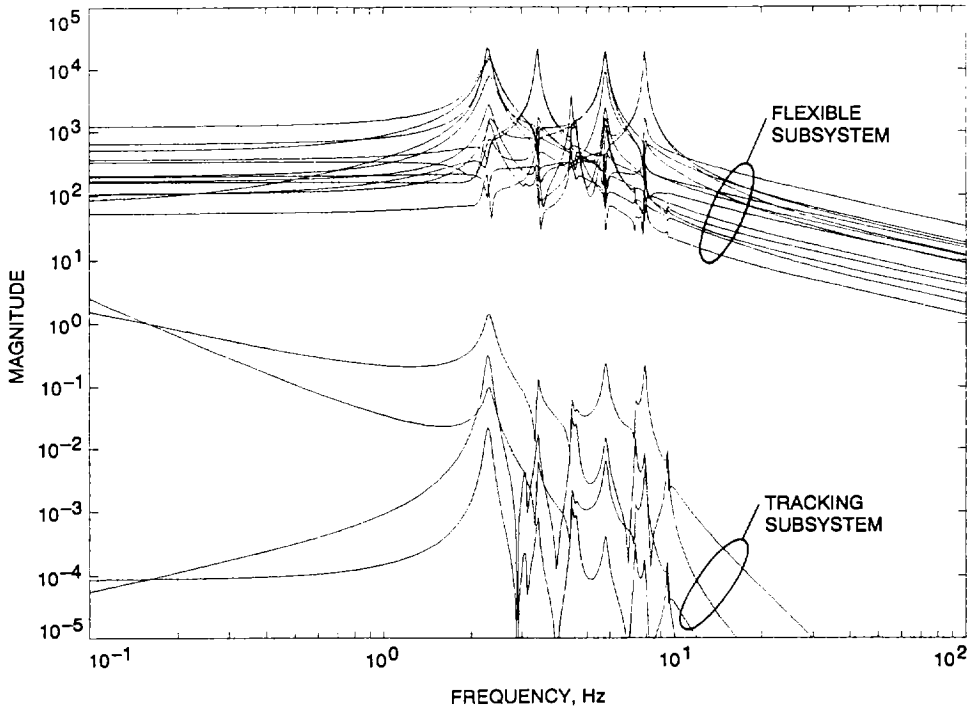

Fig. 3. Magnitudes of transfer function of tracking and flexible subsystems for the elevation rate input.

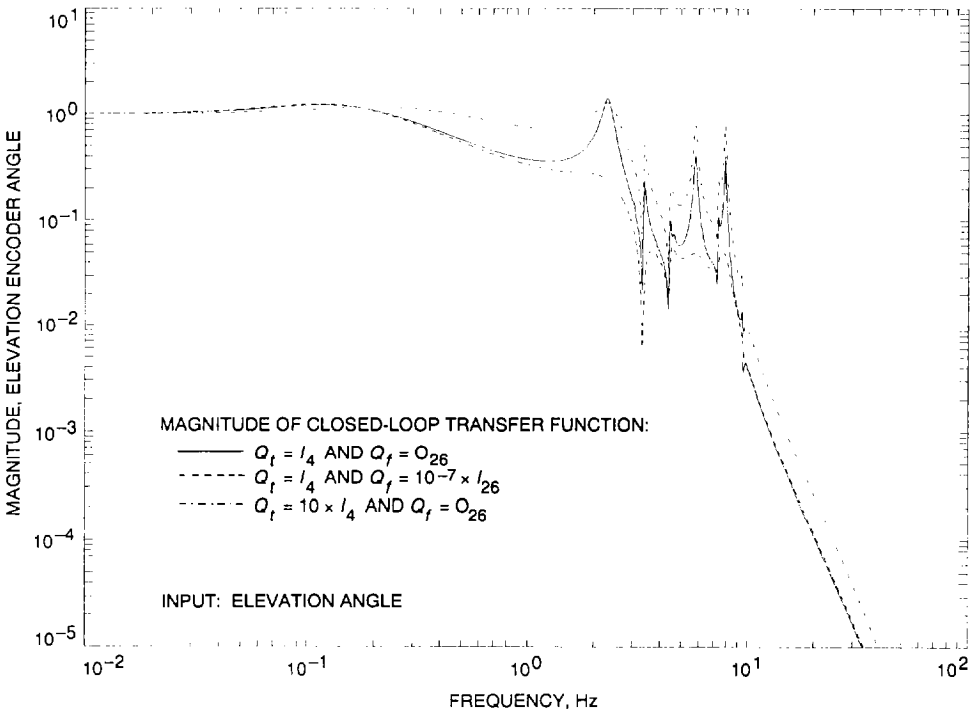

Fig. 4. Magnitudes of transfer function of the closed loop system for different weights of elevation angle to elevation command.

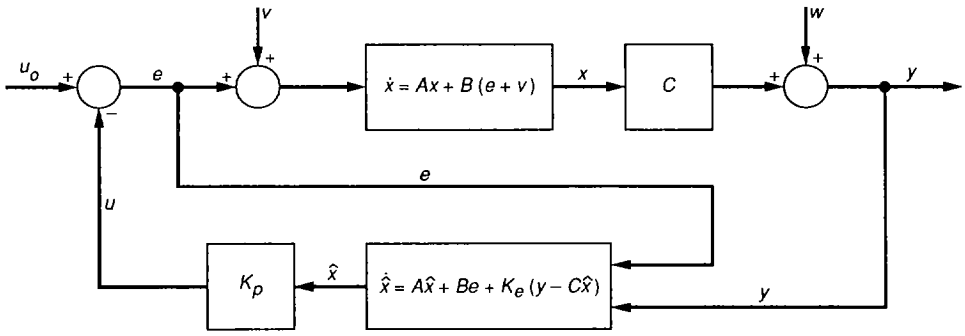

Fig. 5. A flexible structure with an LQG compensator.

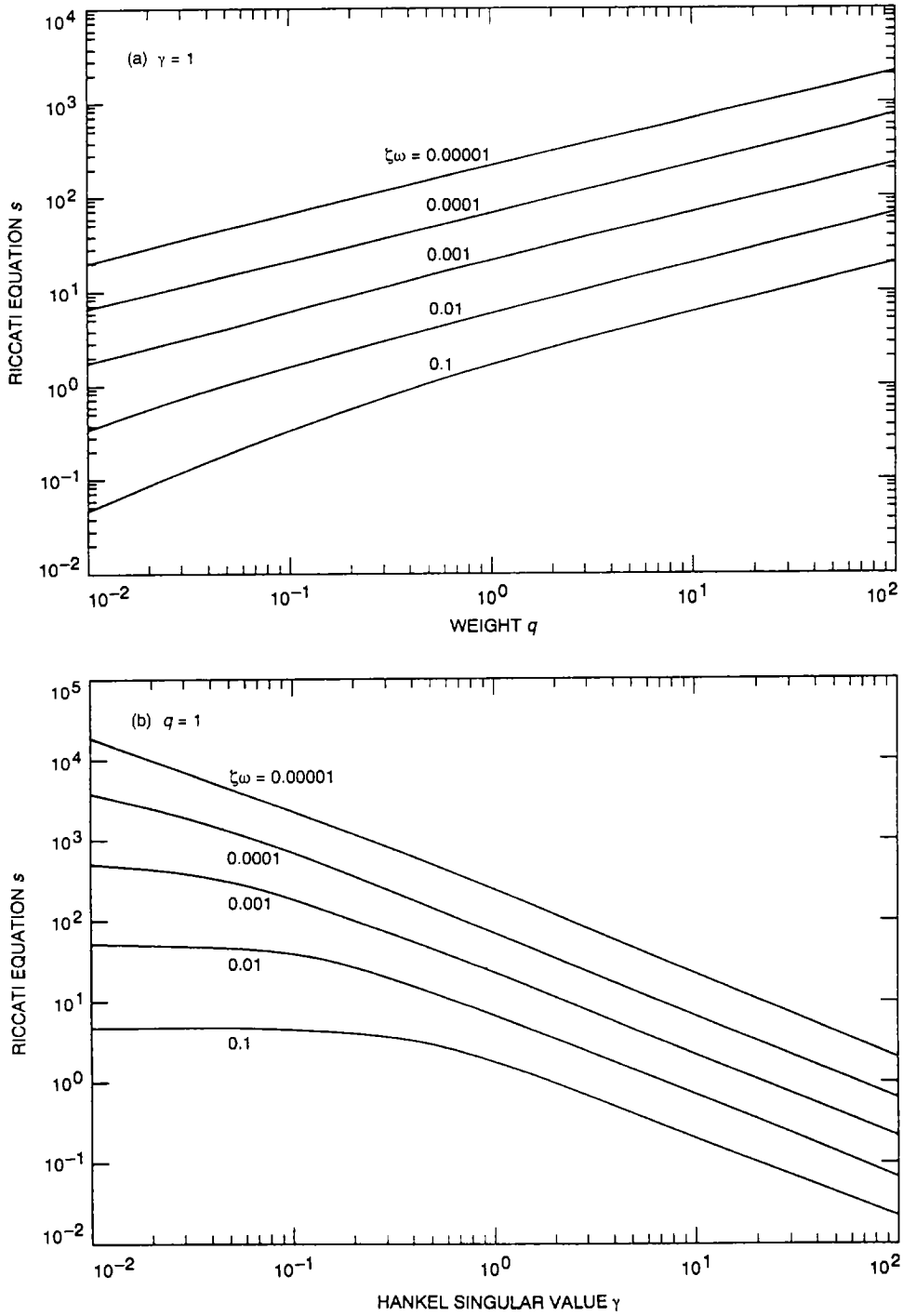

Fig. 6. Solution of the Riccati equation s versus: (a) weight q and (b) Hankel singular value γ.

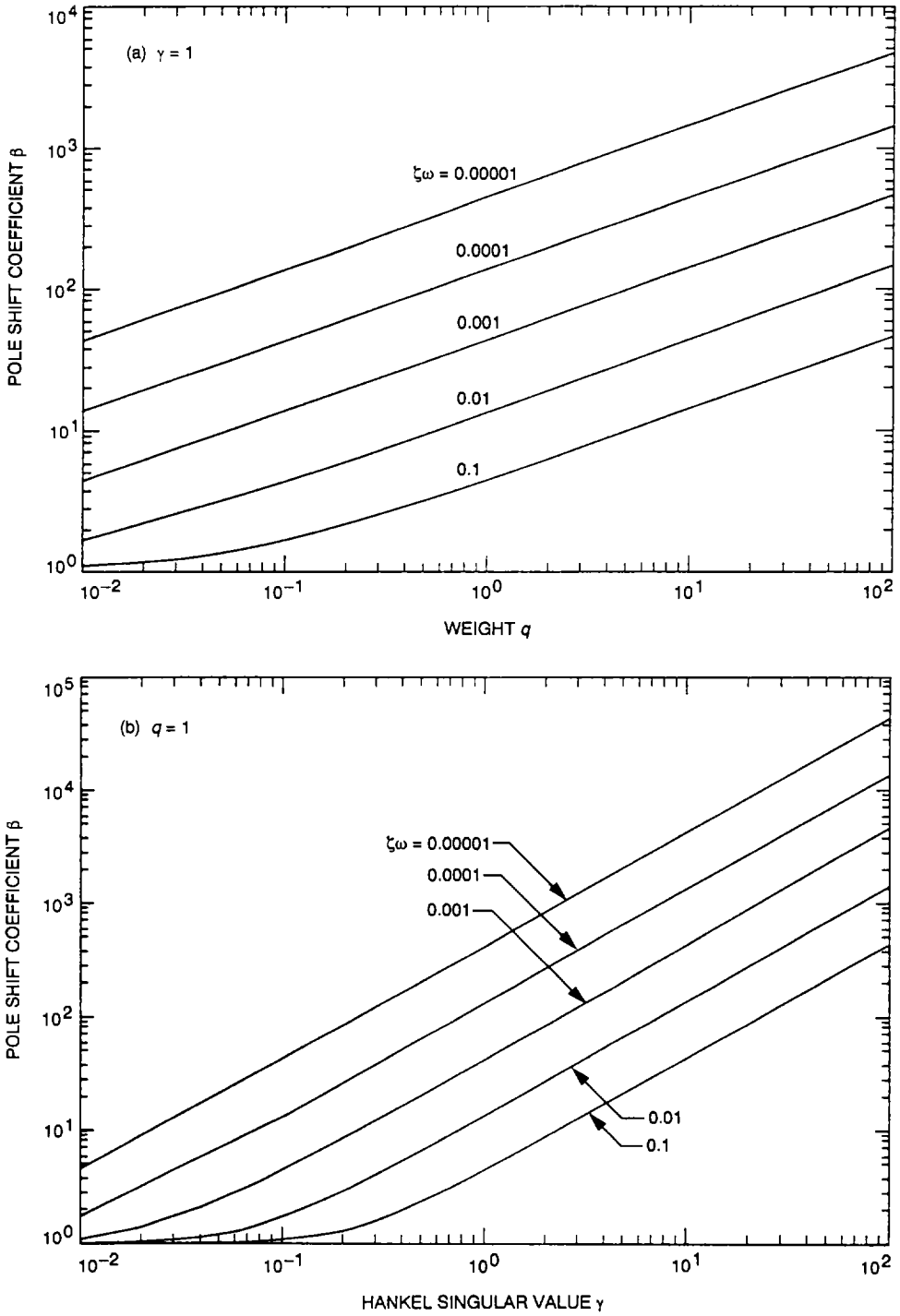

Fig. 7. Pole shift factor β versus: (a) weight q and (b) Hankel singular value γ.

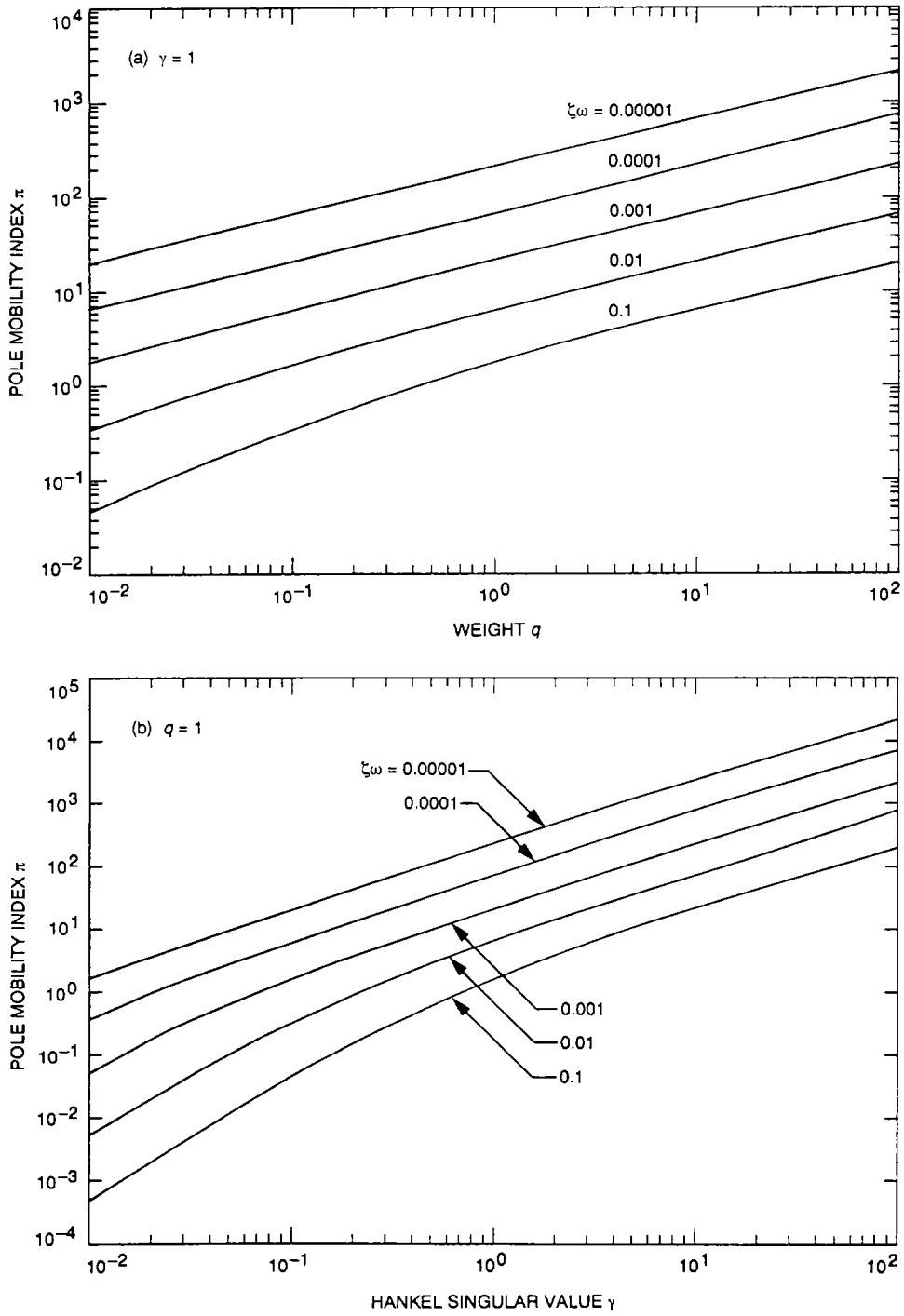

Fig. 8. Pole mobility index π versus: (a) weight q and (b) Hankel singular value γ.

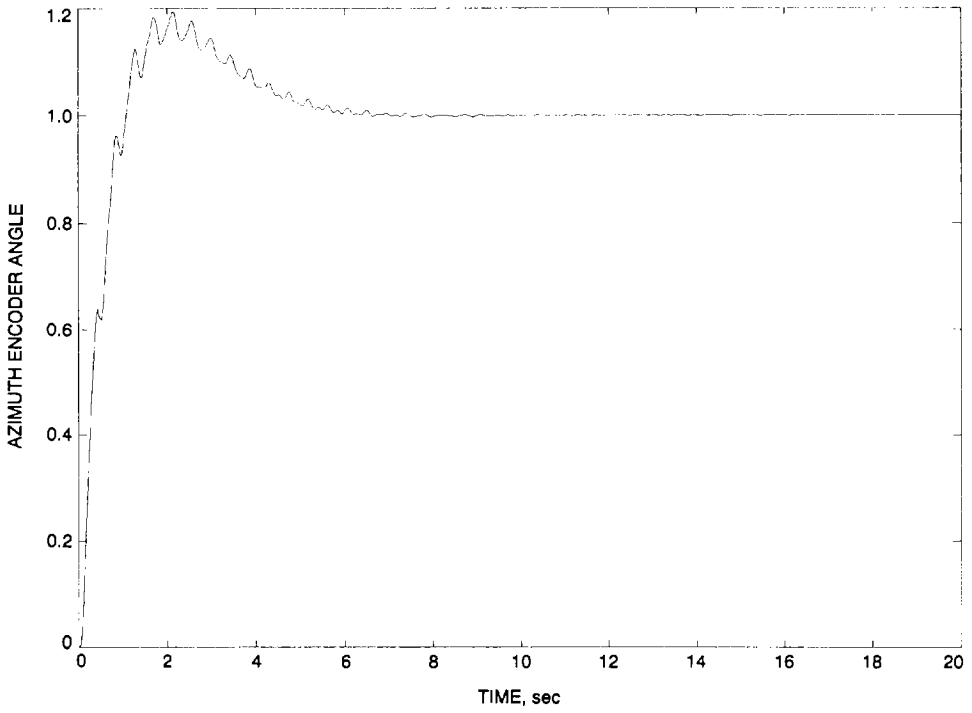

Fig. 9. Azimuth encoder response to azimuth step command for the unit proportional and integral weights in azimuth and elevation, and zero weight for flexible subsystem.

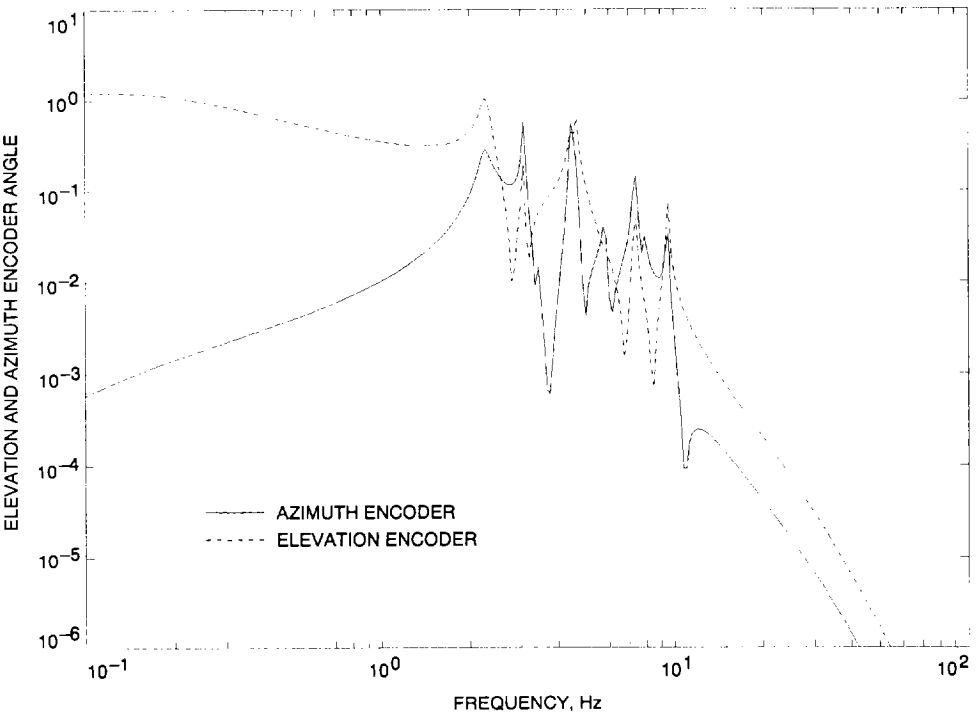

Fig. 10. Transfer function (elevation and azimuth encoder due to azimuth command) for weights the same as those in Fig. 9.

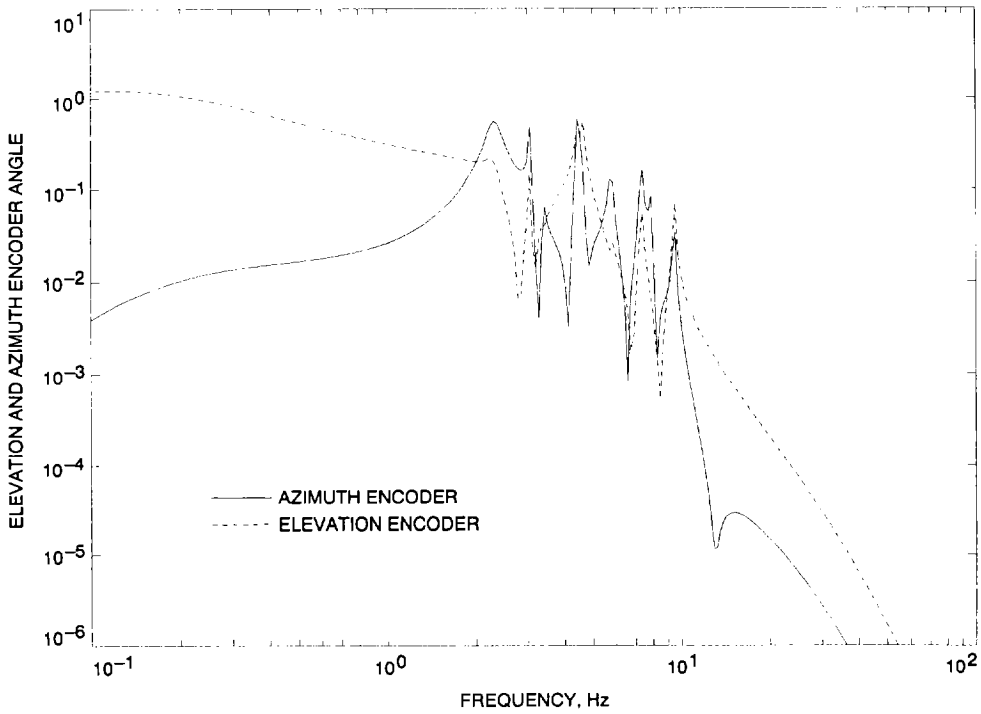

Fig. 11. Transfer function (elevation and azimuth encoder to azimuth command) for weights the same as those in Fig. 9, but for $q_{f1} = 10^{-7}$.

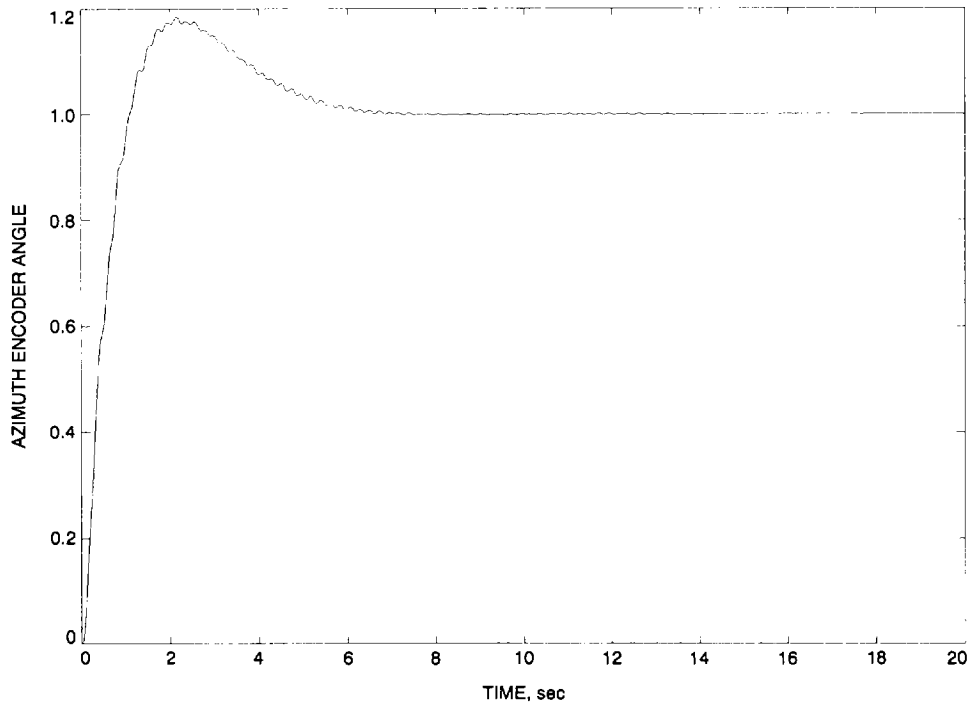

Fig. 12. Azimuth encoder response to azimuth step command for weights the same as those in Fig. 11.

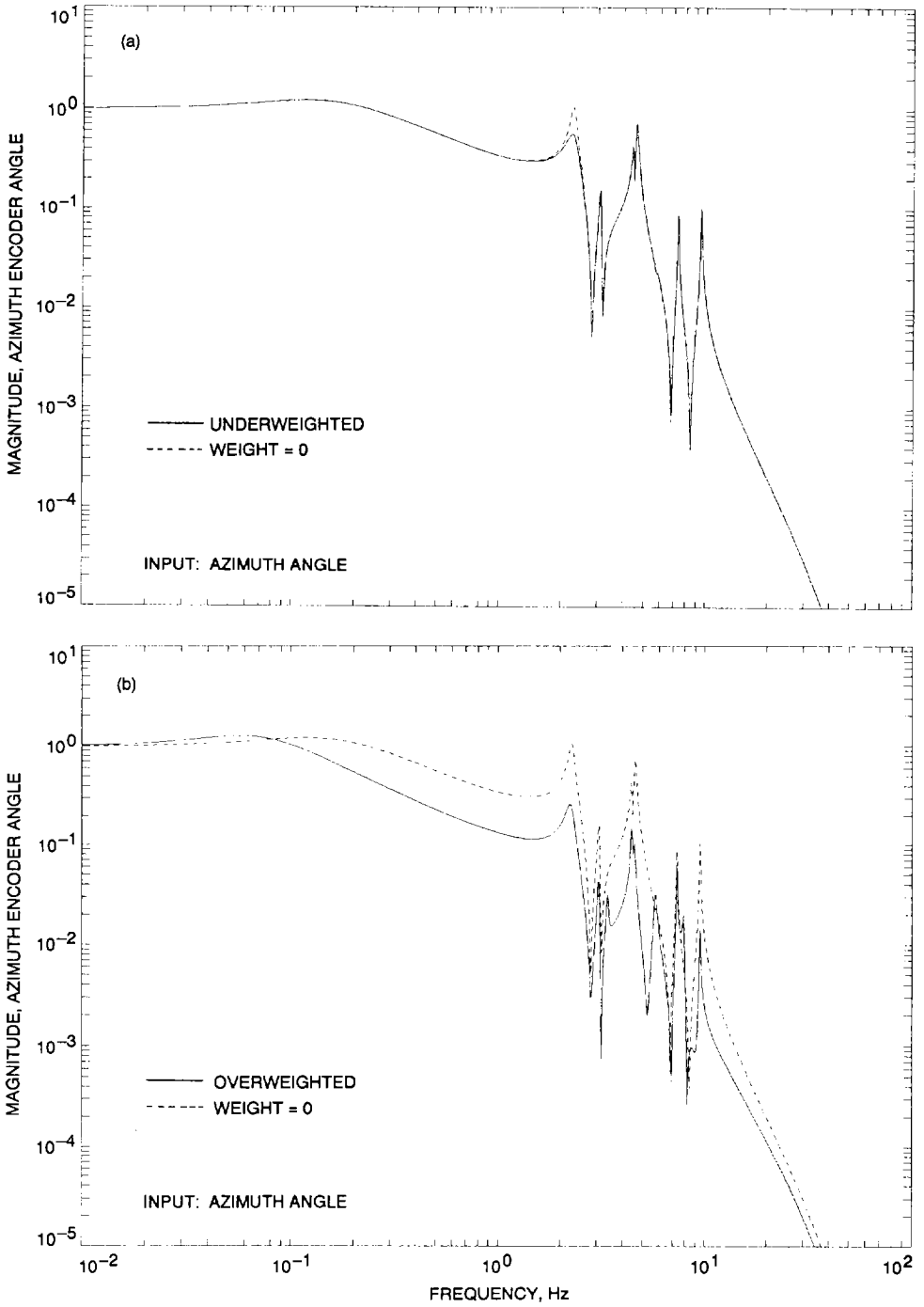

Fig. 13. The first component: (a) underweighted and (b) overweighted.

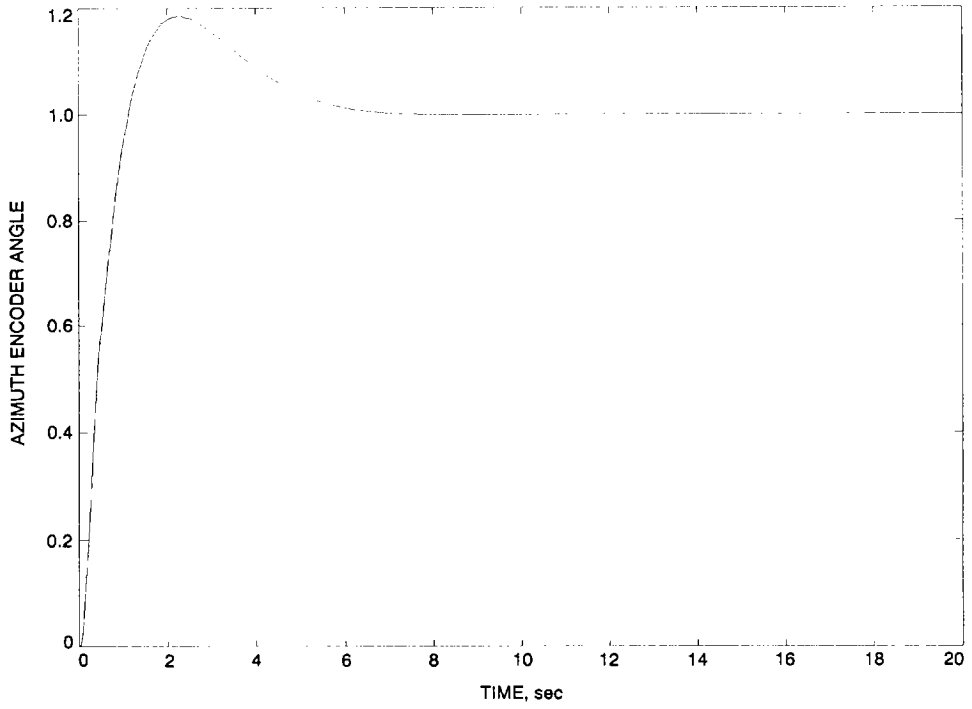

Fig. 14. Azimuth encoder response to azimuth step command for weights the same as those in Fig. 9, but for $q_{f1} = \ldots = q_{f10} = 10^{-7}$.

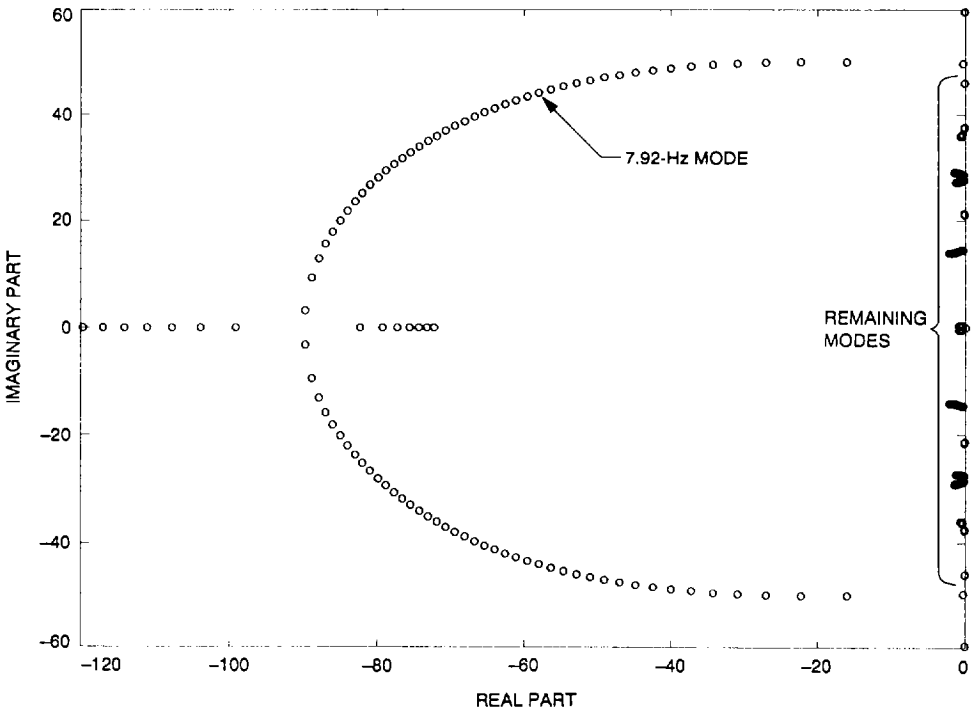

Fig. 15. Root locus for 7.92-Hz mode versus weight.

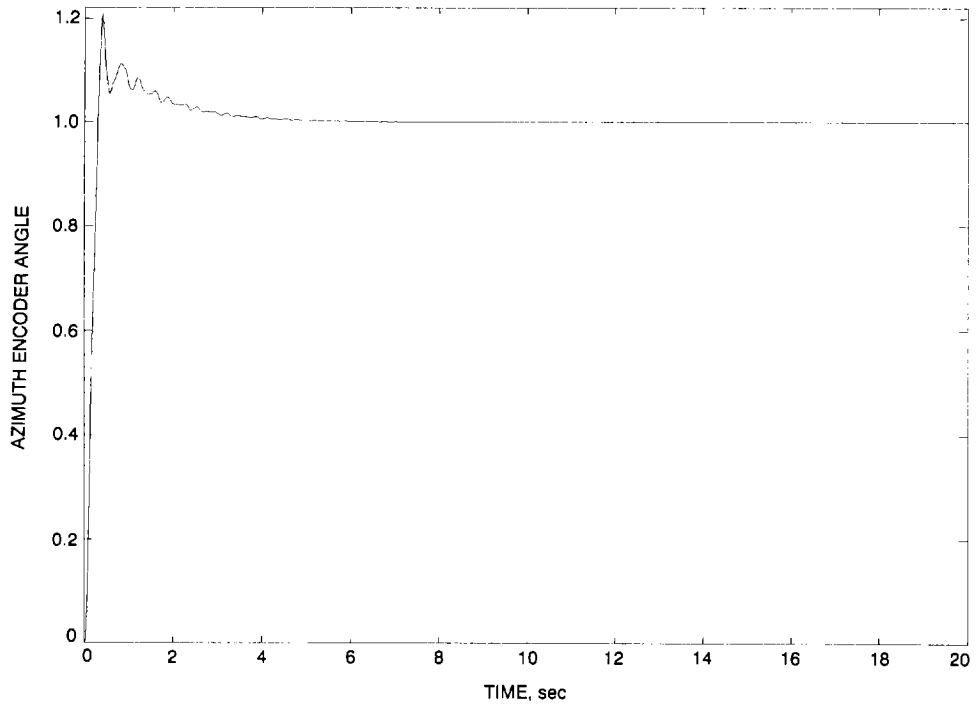

Fig. 16. Closed-loop response to step input for proportional weight 100 and integral weight 70 (both in azimuth and elevation), and weights for flexible subsystem equal to 10^{-7} (azimuth encoder to azimuth command).

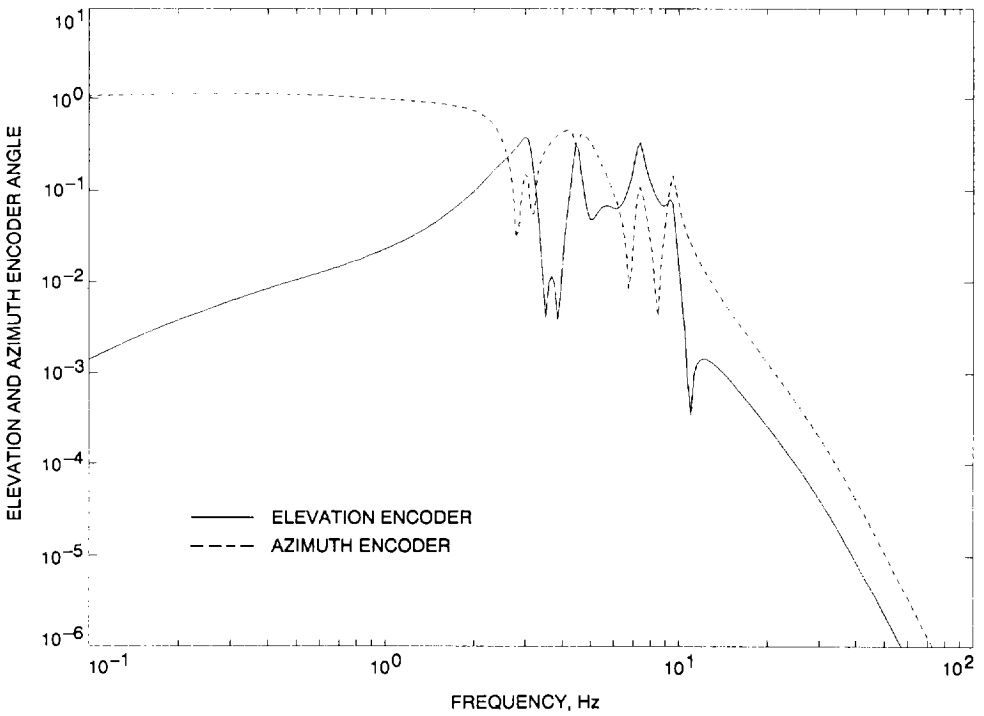

Fig. 17. Closed-loop transfer function for weights the same as those in Fig. 16 (elevation encoder and azimuth encoder to azimuth command).

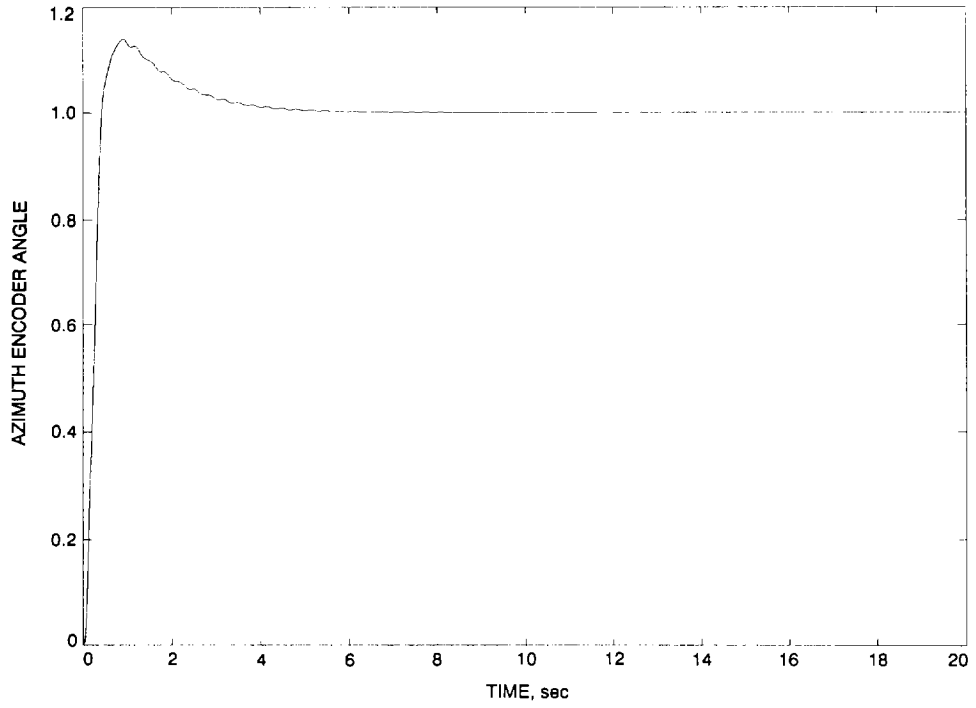

Fig. 18. Azimuth encoder response to azimuth step command for proportional weight 100, integral weight 70 (in azimuth and elevation), and for flexible weights $q_{f1} = \ldots = q_{f6} = 10^{-6}$, $q_{f7} = q_{f8} = 10^{-7}$, and $q_{f9} = q_{f10} = 10^{-5}$.

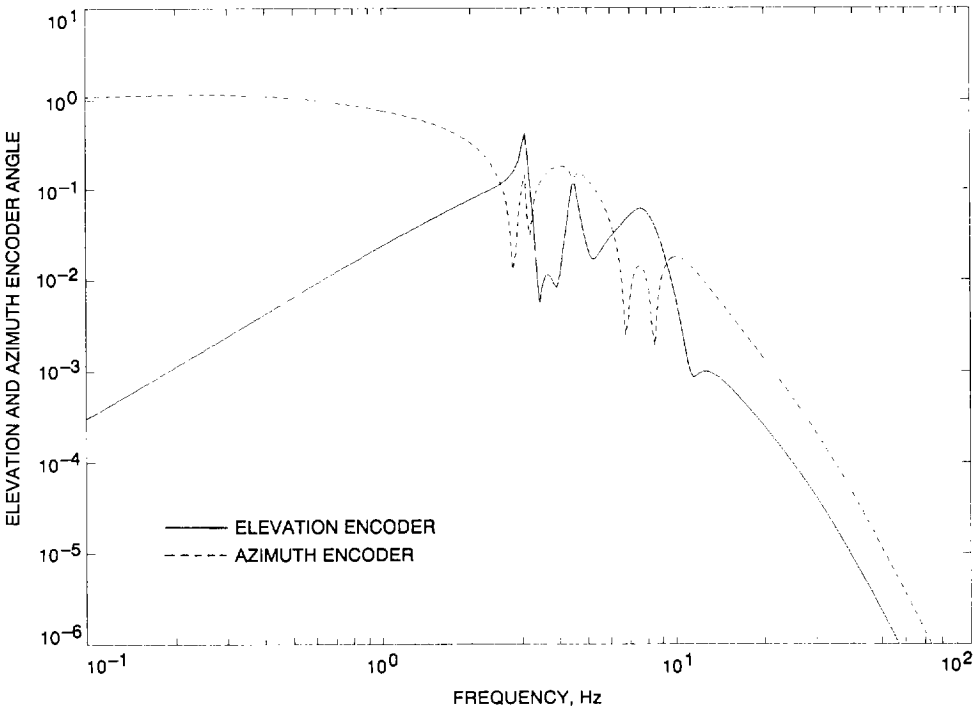

Fig. 19. Closed-loop transfer functions for weights the same as those in Fig. 18 (elevation encoder and azimuth encoder to azimuth command).

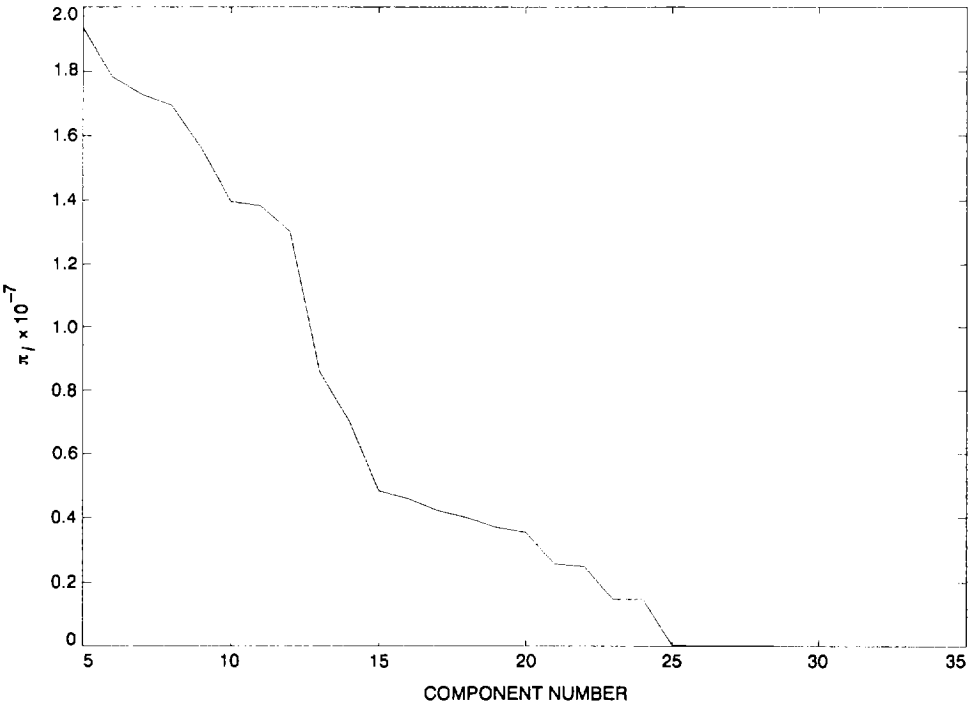

Fig. 20. Pole mobility indices for the DSS-13 antenna.

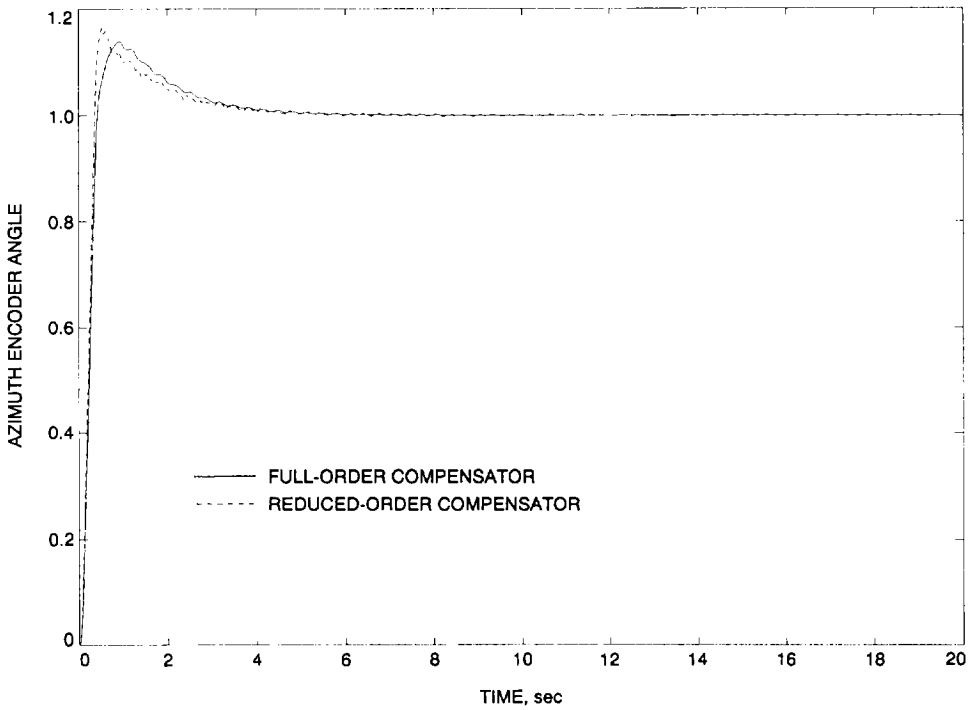

Fig. 21. Step response (azimuth encoder to azimuth command) of the DSS-13 antenna with full- and reduced-order compensators.

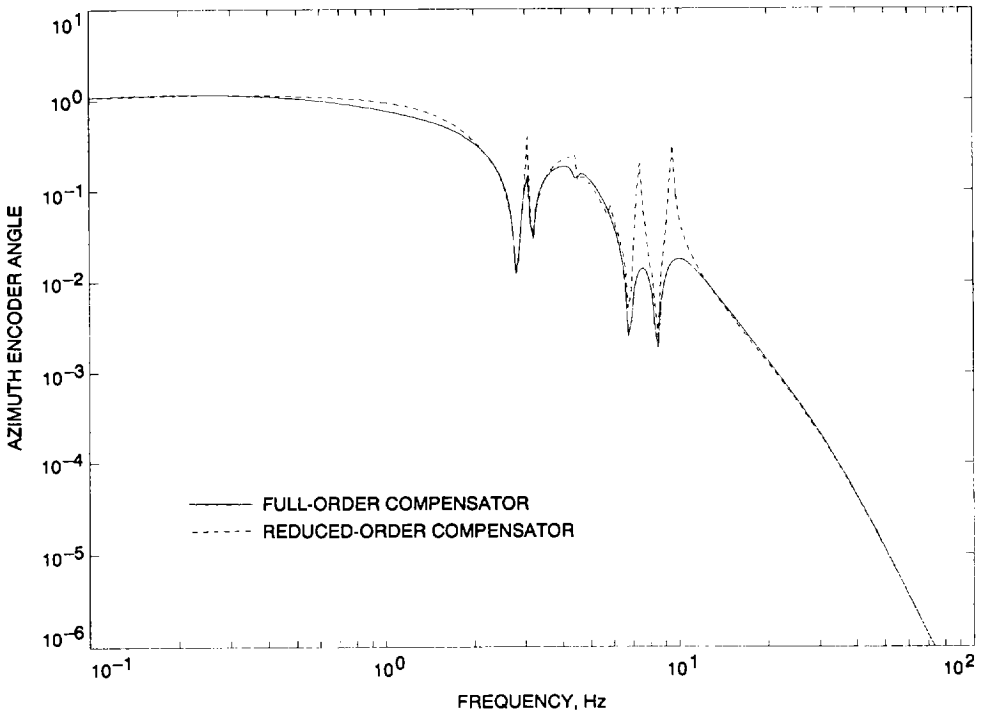

Fig. 22. Transfer function (azimuth encoder to azimuth command) of the DSS-13 antenna with full- and reduced-order compensators.

Appendix

I. Selected Properties of Flexible Systems

The balanced grammian for a flexible system with n components (or $N = 2n$ states) has the following form [7,8]:

$$\Gamma \cong diag(\gamma_1, \gamma_1, \gamma_2, \gamma_2, ..., \gamma_n, \gamma_n) \qquad \text{(A-1)}$$

The system matrix A is almost block diagonal, with dominant 2×2 blocks on the main diagonal:

$$A \cong diag(A_i), A_i = \begin{bmatrix} -\zeta_i\omega_i & -\omega_i \\ \omega_i & -\zeta_i\omega_i \end{bmatrix}, \quad i = 1, ..., n \qquad \text{(A-2)}$$

where ω_i is the ith natural frequency of the structure, and ζ_i is the ith modal damping. The matrices B and C are divided into two blocks, comparably to A, $B^T = [B_1^T, B_2^T, ..., B_n^T]$, and $C = [C_1, C_2, ..., C_n]$, with the following property:

$$B_i B_i^T \cong C_i^T C_i \cong -\gamma_i^2 (A_i + A_i^T) \qquad \text{(A-3)}$$

II. Proof of Eq. (17)

Due to the diagonally dominant matrix A for a flexible structure in balanced representation, and for Q as in Eq. (16), there exists $q_i \leq q_{oi}$, $i = 1, ..., n$, such that the solution S of the Riccati Eq. (4) is also diagonally dominant with 2×2 blocks S_i on the main diagonal:

$$S_i \cong s_i I_2, \quad s_i > 0, \quad i = 1, ..., n \qquad \text{(A-4)}$$

Thus, Eq. (4) turns into a set of the following equations:

$$s_i(A_i + A_i^T) - s_i^2 B_i B_i^T + q_i I_2 = 0, \quad i = 1, ..., n \qquad \text{(A-5)}$$

For a balanced system $B_i B_i^T \cong -\gamma_i^2 (A_i + A_i^T)$ and $A_i + A_i^T = -2\zeta_i\omega_i I_2$, see Eqs. (A-3) and (A-2), respectively. Therefore, Eq. (A-5) is now

$$s_i^2 + s_i/\gamma_i^2 - 0.5 q_i/\zeta_i\omega_i\gamma_i^2 = 0, \quad i = 1, ..., n \qquad \text{(A-6)}$$

There are two solutions of Eq. (A-6), but for a stable system and for $q_i = 0$ it is required that $s_i = 0$, therefore Eq. (17) is the unique solution of Eq. (A-6).

III. Proof of Eq. (23)

For small q_i, the matrix A of the closed-loop system is diagonally dominant $A_o \cong diag\ (A_{oi})$, $i = 1, ..., n$, and $A_{oi} = A_i - B_i B_i^T s_i$. Introducing Eq. (A-3), one obtains

$$A_{oi} \cong A_i + 2 s_i \gamma_i^2 (A_i + A_i^T) \qquad \text{(A-7)}$$

and introducing A_i as in Eq. (A-2) to Eq. (A-7) one obtains

$$A_{oi} = \begin{bmatrix} -\beta_{pi}\zeta_i\omega_i & -\omega_i \\ \omega_i & -\beta_{pi}\zeta_i\omega_i \end{bmatrix} \qquad \text{(A-8)}$$

with β_{pi} as in Eq. (17).

IV. Proof of Eqs. (26a) and (26b)

In order to prove Eqs. (26a) and (26b), the closed-loop Lyapunov equation is considered:

$$(A - BB^T S)\Gamma_c^2 + \Gamma_c^2 (A - BB^T S)^T + BB^T \cong 0 \qquad \text{(A-9a)}$$

or, for the ith pair of variables,

$$(A_i - B_i B_i^T s_i)\gamma_{ci}^2 + \gamma_{ci}^2 (A_i - B_i B_i^T s_i)^T + B_i B_i^T \cong 0 \qquad \text{(A-9b)}$$

Introducing Eq. (A-3) gives

$$\gamma_{ci}^2 + 2\gamma_{ci}^2 \gamma_{oi}^2 s_i - \gamma_{oi}^2 \cong 0 \qquad \text{(A-10)}$$

or

$$\gamma_{oi}^2 / \gamma_{ci}^2 \cong 1 + 2 s_i \gamma_{oi}^2 \qquad \text{(A-11)}$$

Comparing Eq. (A-11) and Eq. (17) gives Eq. (26a).